WARSAW UNIVERSITY OF TECHNOLOGY Index 351733
FACULTY OF CIVIL ENGINEERING
COMMITTEE FOR CIVIL AND WATER ENGINEERING
POLISH ACADEMY OF SCIENCES ISSN 1230-2945

DOI: 10.24425/ace.2020.135220
ARCHIVES OF CIVIL ENGINEERING
Vol. LXVI ISSUE 4 2020

INTERACTION OF RC AND PC CYLINDRICAL SILOS AND TANKS WITH SUBSOIL

P.M. LEWIŃSKI[1]

The subject of this paper is an analysis of the influence of circumferential prestressing on the interaction of cylindrical silos and tanks with the subsoil. The behaviour of the shell structures of RC and PC cylindrical silos or tanks (with circumferential pre-tensioning), and particularly of the ground slab interacting with subsoil, depends largely on the function graphs of the subsoil reactions on the foundation surface. Distributions of the subbase reactions on the ground slab in such structures as silos and tanks have a significant impact on the behaviour of not only the slab itself, but also the interacting shell structure. An analysis of these structures with walls fixed in a circular ground slab and foundation ring was carried out taking into consideration the elastic half-space model using the Gorbunov-Posadov approach and the two-parameter Winkler model. In the computational examples of RC and PC silos and tanks with walls fixed in the circular ground slab or foundation ring, the eventual effects of prestressing obtained as a result of the superposition of internal forces were examined. Although the results for both subsoil models proved to be divergent, the conclusions that follow are fairly important for the engineering practice.

Keywords: silos, tanks, prestressed structures, soil-structure interaction, elastic half-space, Winkler model

[1] DSc., PhD., Eng., Instytut Techniki Budowlanej, ul. Filtrowa 1, 00-611 Warsaw, Poland, e-mail: p.lewinski@itb.pl

1. INTRODUCTION

Design of reinforced concrete and prestressed concrete structures for the storage of bulk materials and liquids is a complex task, demanding a wide range of specialised knowledge and adequate experience. In a number of papers considerations are focused on the effects of loads and prestressing actions with regard to the strains induced by the subsoil reaction on a ground slab due to soil-structure interaction. Ground settlement leading to the deformation and cracking of RC and PC silos and tanks may cause severe damage; therefore special attention is paid to this item. The subject of this paper is an analysis of the influence of subsoil described in the form of an elastic half-space and the Winkler model on the interaction of RC and PC cylindrical silos and tanks with subsoil. In the design calculations of the structure, elastic subsoil models are usually assumed, allowing for the superposition of the actions on structures. The behaviour of the shell structures of PC cylindrical silos or tanks (with circumferential pre-tensioning), and particularly of the ground slab interacting with subsoil, depends largely on the distribution of the subsoil reactions on the foundation surface. Distributions of the subbase reactions on the ground slab in such structures as silos and tanks have a significant impact on the behaviour of not only the slab itself, but also the interacting shell structure. The discussed interactive reactions are described using different models of subsoil, such as the Winkler model, multi-parameter models and the hypothesis of the elastic half-space. This has been the subject of hitherto published papers by many authors, and the utilisation of the last model, supported on the theory of elasticity, was initiated by Borowicka [1], and then developed by Gorbunov-Posadov [4]. However, in the framework of the application of the elastic half-space model for the description of soil-structure interaction, there is a lack of closed solutions for many boundary problems, so it is necessary to use different approximated methods. Some partial results for the proposed model were presented by the author [12] at SSTA-2013 conference. Besides the analytical solution applied further below, there are also used variational formulations and numerical approaches, based on the finite element method and other methods. In the instance of the analytical approaches, methods supported on energy formulations are often used, leading to approximated solutions. In the series of his works, Melerski [16] developed the numerical analysis of tanks using the generalized Winkler model. Girija Vallabhan and Das [3] carried out an analysis of the tank circular ground slab by the finite difference method. Kukreti, Zaman and Issa [9] utilised the principle of minimum potential energy for the determination of the coefficients of the function describing the ground slab deflection. In the instance of the cylindrical tank of varying wall thickness supported on the circular ground slab, Kukreti and Siddiqi [10] used the quadrature method, i.e. an approximated approach,

involving polynomial functions with weights at selected points. Considering a similar problem, Lewiński and Rak [11, 12] used an analytical approach based on the Gorbunov-Posadov method with the convergence control of the power series of the solution for both silos and tanks. The assumed approach gives the advantage of being relatively simple and exact, in relation to common modelling methods. However, in the available literature, this method has not been widely used while the approaches presented there favour Hankel transforms and Bessel function series (see Hemsley [5, 6]) or numerical methods (Melerski [16], Horvath and Colasanti [7], el Mezaini [17], Mistríková and Jendželovský [18]) which lead to complicated algorithms or approximated results. In the computational examples of RC and PC silos and tanks with walls fixed in the circular ground slab or foundation ring, the eventual effects of prestressing obtained as a result of the superposition of internal forces were examined.

2. ANALYSIS OF SOIL-STRUCTURE INTERACTION

For the analytical purposes, we assume that the slab perfectly adheres to the surface of the subsoil which has the properties of the elastic half-space, the slab acts on the subsoil without the friction and perfectly adheres to the subsoil even when is beeing torn off (in the case of concrete tanks, this phenomenon is not observed). In order to attain the solution in the instance of an elastic and isotropic half-space loaded on the certain domain of the limiting plane in a perpendicular way, the influence surface is used (the Green function), i.e. by using the *Boussinesq* solution obtained for arbitrary located vertical force P acting on the isotropic half-space [1, 4]. According to this solution, the vertical displacement of the limiting plain ($z = 0$) amounts:

$$v\big|_{z=0} = \frac{P\left(1-\nu_0^{\,2}\right)}{\pi E_0 r} \tag{2.1}$$

where E_0 and ν_0 are modulus of elasticity and Poisson ratio of the elastic half-space, while r is a distance of the considered point from the point of the application of the concentrated force P. Considering the instance of the loading of such a half-space by the pressure transmitted through a circular slab in a perpendicular way, we assume that the axi-symmetric loading $p(r)$ operates on it – at the same time this is a function describing the half-space reaction on the slab.

Let us introduce the non-dimensional variables: ρ, $\overline{\rho}$, α and χ such that:

ρ – non-dimensional distance from the centre of the slab to the point of the surface of the subsoil, in which the displacement is evaluated ($\rho = r/R$, where r – a real distance, R - the slab radius),

$\bar{\rho}$ – non-dimensional distance from the slab centre to the point of the application of the load,

α – non-dimensional radius of the loading q, $\alpha = a / R$, where: a – the loading radius (Figure 1),

χ – arbitrary parameter of integration.

The Green function is integrated over the surface of the circular slab. The elastic subsidence of half-space, $v(\rho)$, from the load $p(\rho)$ transmitted by the circular slab (see [13]), can be given in the form:

$$v(\rho) = \frac{4(1-\nu_0^2)R}{\pi E_0}\left\{\frac{1}{\rho}\int_0^{\rho}\left[p(\bar{\rho})\bar{\rho}\int_0^{\frac{\pi}{2}}\frac{\mathrm{d}\chi}{\sqrt{1-\left(\frac{\bar{\rho}}{\rho}\right)^2\sin^2\chi}}\right]\mathrm{d}\bar{\rho} + \int_{\rho}^{\alpha}\left[p(\bar{\rho})\int_0^{\frac{\pi}{2}}\frac{\mathrm{d}\chi}{\sqrt{1-\left(\frac{\rho}{\bar{\rho}}\right)^2\sin^2\chi}}\right]\mathrm{d}\bar{\rho}\right\} \tag{2.2}$$

As the subsoil reaction on the slab acts on its whole bottom surface, the parameter $\alpha = 1$ $(a = R)$.

The differential equation of the circular slab resting on the elastic half-space and subjected to loading q, uniformly distributed on the surface of the circle of the radius a (Fig. 1), takes the form:

$$\frac{\mathrm{d}^4 w}{\mathrm{d}\rho^4} + \frac{2}{\rho}\cdot\frac{\mathrm{d}^3 w}{\mathrm{d}\rho^3} - \frac{1}{\rho^2}\cdot\frac{\mathrm{d}^2 w}{\mathrm{d}\rho^2} + \frac{1}{\rho^3}\cdot\frac{\mathrm{d}w}{\mathrm{d}\rho} = \frac{R^4}{D}[q - p(\rho)] \tag{2.3}$$

where D is a bending stiffness of the slab.

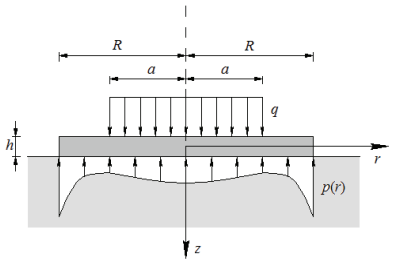

Fig. 1. The scheme of the circular slab on the elastic half-space.

The displacements of the surface of the elastic half-space and the displacements of the slab must be identically equal: $v(\rho) \equiv w(\rho)$. The function $p(\rho)$ of the interaction between the slab and elastic half-space, can be assumed in the form of the polynomial:

$$p(\rho) = \sum_{n=0}^{\infty} a_{2n} \rho^{2n} \tag{2.4}$$

In order to evaluate the integral of the equation (2.3), at first we can consider the homogeneous equation. Its solution constitutes the function:

$$w_o = C_1 \rho^2 \ln \rho + C_2 \rho^2 + C_3 \ln \rho + C_4 \tag{2.5}$$

where C_i, $i = 1...4$ are the constants of integration. The particular integral of the equation (2.3) can be sought in the form:

$$w_s = \sum_{n=2}^{\infty} A_{2n} \rho^{2n} \tag{2.6}$$

The coefficients A_{2n} may be expressed by the components a_{2n} of a series (2.4) by substituting this series to the Eqn. (2.3) and comparing the components of identical powers. This gives a set of algebraic N equations (in the above series $N = \infty$), to which the equilibrium equation of the slab loadings should be added first. The full solution can be obtained by adding the particular integral to the Eqn. (2.5). Eventually, the slab deflection in the area of the action of the loading q (which is denoted by the index I) is expressed by the equation:

$$w_I = C_{1,I} \rho^2 \ln \rho + C_{2,I} \rho^2 + C_{3,I} \ln \rho + C_{4,I} + \frac{R^4}{64D}(q - a_0)\rho^4 - \frac{R^4}{16D} \sum_{n=1}^{N} \frac{a_{2n}}{(n+2)^2 (n+1)^2} \rho^{2n+4} \tag{2.7}$$

The constants $C_1,...,C_4$ are determined from the conditions in the centre and at the boundaries of the slab. Moreover, substituting the expression of the interaction function (2.4) into the equation of the vertical displacement of the subsoil surface (2.2), expressing both elliptic integrals by the hypergeometric series, and then performing the multiplication and integration of the series, the equation for the vertical displacements of the half-space can also get a form of a power series.

$$v(\rho) = \frac{2(1-v_0^{\,2})R}{E_0}\left\{\sum_{n=0}^{N}\sum_{m=0}^{\infty}\left[\frac{\prod_{k=0}^{m}(2k-1)}{2^m m!}\right]^2 \frac{a_{2n}}{2n-2m+1}\rho^{2m}\right\} \tag{2.8}$$

By identifying $v(\rho) \equiv w(\rho)$, the coefficients of the series at the equal powers of ρ can be compared, which leads to a set of N algebraic equations, allowing for the evaluation of the coefficients a_{2n}. In practical calculations during the determination of the expressions a_{2n} the convergence of the solution is examined and in this way the number N is defined. In the surrounding of the circle of radius $r = R$, stress concentration can be encountered (as it is a contact problem), and therefore the function $p(\rho)$ can pursue infinity. Thus, if this function were expressed by the infinite power series, this would have been divergent at this point. Next, there should be included the instance of the actions of the moments on the slab circumference as well as radial and shear forces through the formulation of proper boundary conditions. To perform the comparative calculations of the ground slab of the tank, the model of the circular slab resting on the two-parameter Winkler foundation model (taking into account the vertical subgrade reaction modulus $k_1 = K_z$ and the horizontal one $k_2 = K_t$) was used herein (see [8]).

3. INTERACTION OF RC AND PC SILOS WITH SUBSOIL

3.1. INTERACTION OF THE CYLINDRICAL SILOS WITH SUBSOIL

In the analysis of the soil-structure interaction of axisymmetrical silos the theory of boundary perturbations was used (see the textbooks [2,15]). The conditions of applicability of this theory are fulfilled. In order to perform the analysis of the pre-tensioning effect, a circular RC grain silo (A) consisting of a cylindrical shell fixed in the circular ground slab was considered (see Fig. 2 a)). The slab was resting on the subsoil modelled by both models described above. The silo structure was loaded axi-symmetrically by the Janssen-type pressure. A particular integral of the displacement equation of the cylindrical shell loaded in this way can be predicted in a form connected with the loading function (see the textbook [19]). The following silo parameters were adopted: mean radius R = 7 m, height H = 40 m, wall thickness h = 20 cm and the ground slab thickness: h_d = 80 cm, while the reinforced concrete gravity γ_c = 25 kN/m^3. The following load variants were considered: the bulk material pressure and the adequate loading of ground slab and the dead weight of the silo wall together

with the the bulk material friction, and subsequently - the effect of pre-tensioning. In order to compare objectively the results obtained with the assumption of an elastic half-space and two-parameter Winkler model, the dead weight of the slab was omitted, because the ground slab undergoes deformation under its dead weight at the concrete laying stage. For the sake of clarity, the influence of standard coefficients was also omitted.The following material data were assumed: elastic modulus of concrete: $E_c = 31$ GPa, Poisson ratio of concrete: $\nu_c = 0.2$, the elastic modulus of the subsoil – an elastic half-space: $E_0 = 280$ MPa, Poisson ratio of the subsoil: $\nu_0 = 0.3$, as well as the vertical subgrade reaction modulus: $K_z = 25$ MN/m^3 and the horizontal subgrade reaction modulus: $K_t = 5$ MN/m^3 of the two-parameter Winkler model. In order to determine the grain pressure it was assumed that the grain gravity: $\gamma_z = 8$ kN/m^3, the coefficient of lateral pressure: $K = 0.59$, the frictional coefficient of grain against the vertical silo wall: $\mu = 0.24$. Computation was performed and the plots were drawn taking into account $N = 100$ first terms of the series expansion of the soil-structure interaction function. This assumption ensures sufficient accuracy of the solution (see [12–14]).

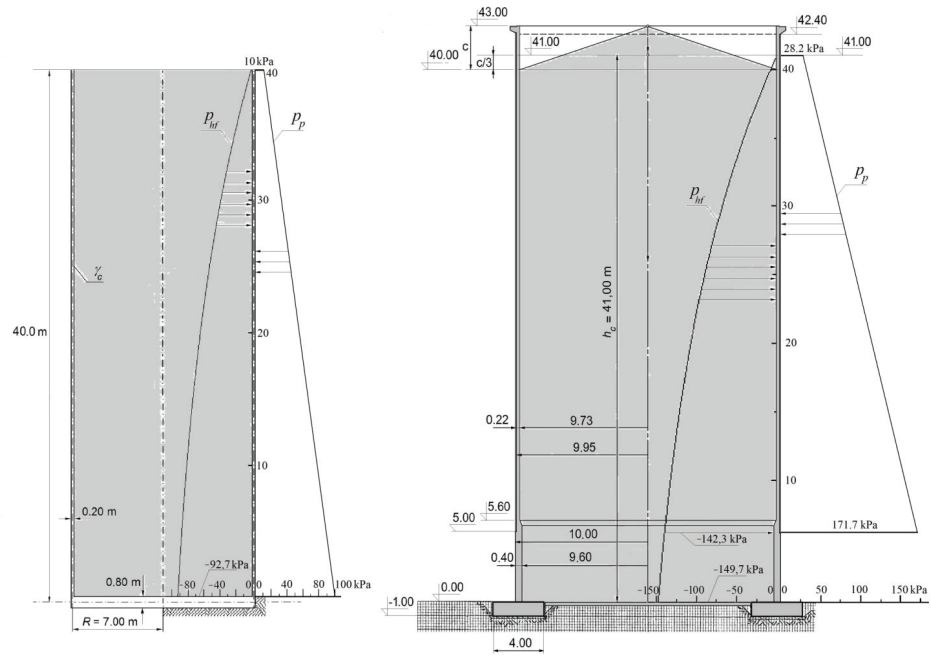

a) b)

Fig. 2. The axi-symmetrical concrete silos: a) grain silo A, b) aluminium oxide silo B.

The plots of displacements and stress resultants as well as the functions of subsoil reactions have been evalueated. However, only the graphs of internal forces in the silo's shell from the horizontal pressure p_{hf} for the substrate models of the elastic half-space and two-parameter Winkler springs are presented. The distributions of the circumferential force N_ϑ and the meridional moment M_z in the silo A's shell are shown in Figures 3a) and 3b), respectively.

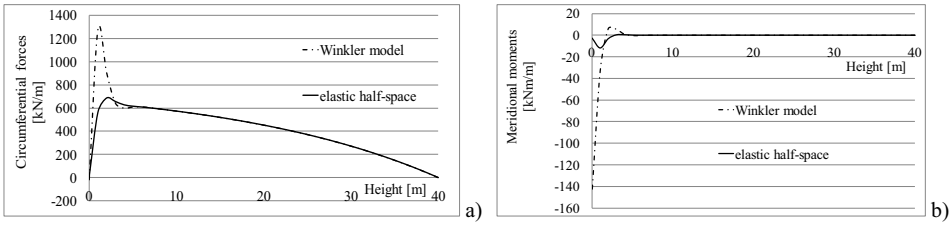

Fig. 3. Plots of circumferential forces N_ϑ (a)) and meridional moments M_z (b)) in the silo A's wall due to the Janssen-type pressure (p_{hf}) for the subsoil models of elastic half-space and two-parameter Winkler model.

Afterwards, the case of the pre-tensioned cylindrical silo shell resting on the foundation ring was analyzed (silo B). The cross-section of the wire-wound circular silo bin (B) of variable thickness for the storage of aluminium oxide with walls fixed in the RC ring is shown in Fig. 2 b). Its static scheme corresponds to this figure. The following geometric data were adopted: silo height: $h_c = 41$ m; upper and lower shell height: 36 m and 5 m, respectively; inner radii of the upper and lower shell: 9.73 m and 9.60 m, respectively; wall thicknesses of the upper and lower shell: 0.22 m and 0.40 m, respectively; height and width of the foundation ring: 1 m and 4 m, respectively. Material data adopted for the calculation are: elasticity moduli of the cylindrical shell the foundation ring: 20 GPa and 16 GPa, respectively, Poisson's coefficient of concrete: $\nu_b = 0.18$, elastic modulus of subsoil: $E_0 = 92.7$ MPa, Poisson's coefficient of subsoil: $\nu_0 = 0.3$. The vertical subgrade modulus of the Winkler foundation was determined taking into account the attachment of the silo shell in the elastically supported foundation ring. The subgrade vertical modulus ($K_z = C_z$) can be calculated according to consistent formula for the foundation rings on the subgrade of elastic half-space [13]:

$$C_z = \frac{3\pi}{4b}\frac{E_0}{1-\nu_0^2}, \tag{3.1}$$

where b is the width of the foundation ring. Assuming moduli E_0 and ν_0, and b as above, the subgrade modulus $K_z = 60$ MN/m^3 is obtained, which corresponds to soils of relatively high stiffness.

Considering the Janssen-type actions on a structure it was assumed that: specific weight of the bulk material: 10 kN/m^3, $K = p_h/p_v = 0.455$, the friction coefficient between the material and the wall: $\mu = 0.404$ and partial factor for variable actions $\gamma_Q = 1{,}5$. Using the proprietary software, a computational analysis of the internal pressure was carried out. Figures 4a) and b) present the diagrams of the hoop force N_ϑ and meridional moment M_z in the shell from the horizontal pressure.

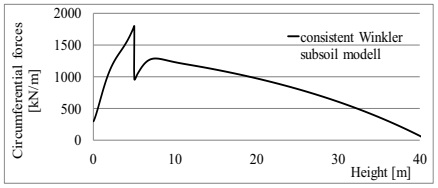

a)

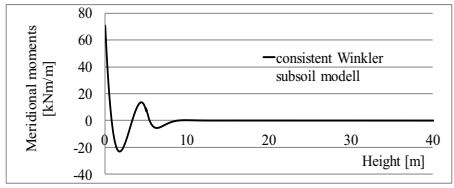

b)

Fig. 4. Distributions of circumferential forces N_ϑ (a)) and meridional moments M_z (b)) in the silo B's wall due to the Janssen-type pressure (p_{hf}) for the consistent Winkler subsoil model.

3.2. EFFECT OF PRESTRESSING ON THE SILO FIXED IN GROUND SLAB

The second example deals with the wire-wound circular PC silo A (see Fig. 2 a)) and its stress resultants from the trapezoidal-shaped normal radial pressure of pre-tensioning. It was assumed that the radial pressure from the prestressing at the top is p_{pg} =10 kPa while at the bottom it is p_{pd} =100 kPa. The graphs depicting the distributions of the circumferential force N_ϑ and the meridional moment M_z in the silo A's shell as the effects of prestressing pressure taking into account soil-structure interaction for the subsoil models of the elastic half-space and 2-parameter Winkler springs are shown in Fig. 5.

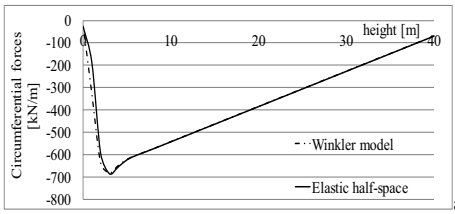

a)

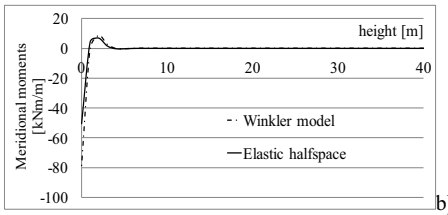

b)

Fig. 5. Distributions of the circumferential forces N_ϑ (a)) and meridional moments M_z (b)) in the silo A's wall from the pre-tensioning for the elastic half-space and two-parameter Winkler model.

The graphs of the stress resultant distributions, i.e. the circumferential force N_ϑ and the meridional moment M_z in the silo shell from the combined horizontal pressure (p_{hf}) and the pre-tensioning for the subsoil models of the elastic half-space and two-parameter Winkler model are shown in Fig. 6.

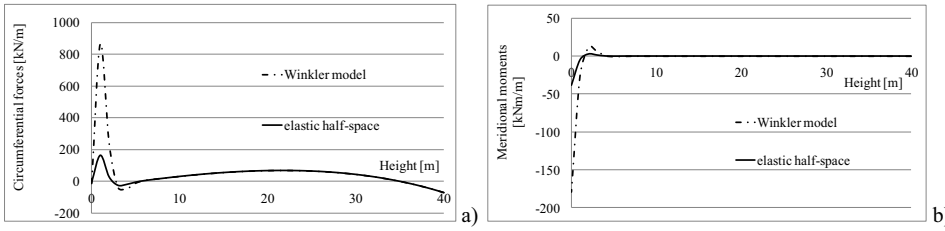

Fig. 6. Plots of hoop forces N_ϑ (a)) and meridional moments M_z (b)) in the silo A's from the internal pressure and pre-tensioning for the subsoil models of the elastic half-space and two-parameter Winkler model.

The graph in Fig. 6a) is not a superposition of graphs in Figures 3a) and 5a), as well as the graph in Fig. 6b) is not a superposition of graphs in Figures 3b) and 5b), because all the graphs concerning individual load cases (Janssen-type pressure, pre-tensioning) were prepared including the dead weight of the silo wall, which was taken into account once in the superposition.

3.3. EFFECT OF PRESTRESSING ON THE SILO FIXED IN THE RING

The pre-tensioning actions on the surface of the cylindrical silo B's shell fixed in the foundation ring were analyzed (see Fig. 2 b)). The effective radial pressure from the wire-winding was assumed as the trapezoidal normal pressure for the upper cylindrical shell; the radial pressure at the top: 28.2 kPa, while at the bottom: 171.7 kPa. The wire-wound pre-tensioning is applied above the level of +5.00 m. Using the proprietary software, a computational analysis of pre-tensioning effect was carried out.

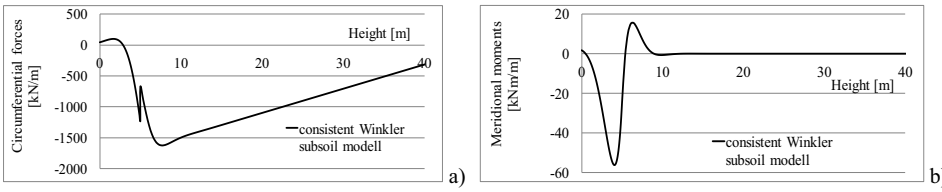

Fig. 7. Distributions of circumferential forces N_ϑ (a)) and meridional moments M_z (b)) in the silo B's wall from the prestressing pressure for the consistent Winkler subsoil model.

The diagrams which present the distributions of the circumferential forces N_ϑ and the meridional moments M_z in the silo B's shell from the pre-tensioning are shown in Fig. 7a) and b). The resultant distributions of the effects of the actions on the silo which present the distributions of the circumferential forces N_ϑ and the meridional moments M_z in the silo B's shell from the combined horizontal pressure (p_{hf}) and the trapezoidal pre-tensioning pressure are shown in Fig. 8a) and b).

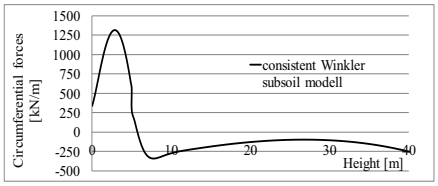

a)

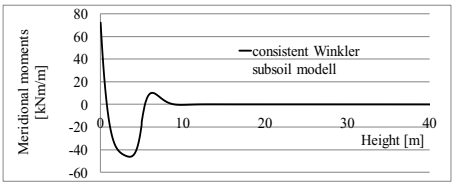

b)

Fig. 8. Distributions of circumferential forces N_ϑ (a)) and meridional moments M_z (b)) in the silo B's shell from the combined horizontal pressure (p_{hf}) and prestressing pressure.

4. INTERACTION OF RC AND PC TANKS WITH SUBSOIL

4.1. INTERACTION OF THE CIRCULAR WATER TANK WITH SUBSOIL

Basing on the above described algorithm, the behaviour of the RC cylindrical tank subjected to different variants of axi-symmetrical load was analyzed taking into account two substrate models, i.e. an elastic half-space and two-parameter Winkler model. A water tank made of concrete with elasticity modulus: 31 GPa and Poisson ratio: 0.2 was assumed, consisting of a cylindrical shell with an average radius of 7.0 m, a height of 5.0 m and a thickness of 20 cm, connected to a circular ground slab 20 cm thick. The ground in the substrate with: E_0 = 280 MPa and ν_0 = 0.3 was assumed. In the comparative calculations for the Winkler foundation, two subgrade moduli were adopted: vertical (C_z = 25 MN/m^3) and the horizontal (C_t = 5 MN/m^3). The geometry of the tank in a vertical cross-section is shown in Fig. 9. A few load variants were considered herein, taking into account the hydrostatic pressure (the liquid specific weight was assumed to be 10 kN/m^3), the loading of the ground slab with the liquid (p_v = 50 kPa) and the dead weight of the wall per unit of the circuit: $P = \gamma_c \cdot l \cdot h =$ 25 kN/m. In order to obtain a more impartial comparison of the results obtained with the assumption of the elastic half-space model and the two-parameter Winkler foundation, the dead weight of the ground slab in this example was omitted as in the instance of the RC silo (see p. 3.1). For the series describing

the interaction of the ground slab with soil and providing sufficient accuracy, the first 100 terms of expansion were taken into account.

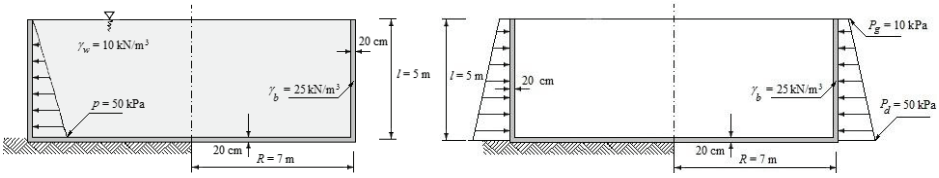

Fig. 9. The circular tank filled with water and the horizontal pressure with trapezoidal distribution.

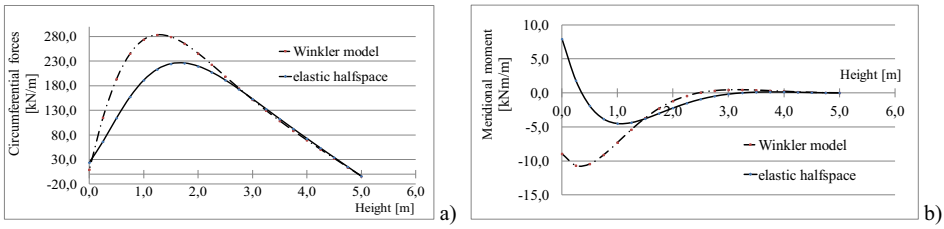

Fig. 10. Distributions of circumferential forces N_ϑ (a)) and meridional moments M_z (b)) in the tank wall from the hydrostatic pressure for subsoil models of the elastic half-space and the two-parameter Winkler model.

The linear relationship between peripheral forces and radial displacements of tank walls causes the graph of these displacements have the form analogous to the plot of peripheral forces (Fig. 10a)).

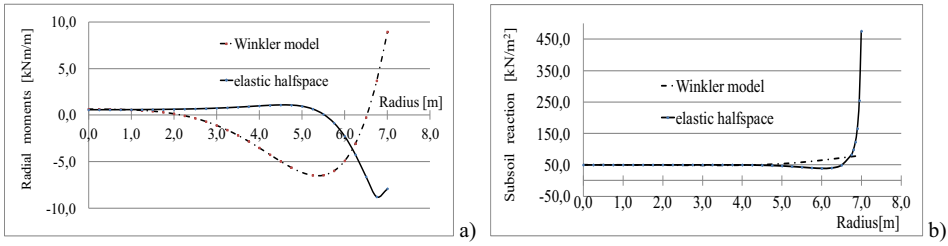

Fig. 11. Distributions of radial moments M_r (a)) in the ground slab from the water pressure and the subsoil reaction (b)) for the subsoil models in the form of the elastic half-space and two-parameter Winkler model.

A similar analogy occurs between the plot of meridional moments (Fig. 10b)) and latitudinal moments in the tank wall, so there is no need to include charts of these displacements and latitudinal moments. Figure 11a) shows the radial moment distributions in the ground slab of the reservoir and Fig. 11b) –

the reactions of the substrate under the ground slab in the case of the application of the substrate models in the form of the elastic half-space and the Winkler model.

4.2. EFFECT OF PRESTRESSING ON THE TANK FIXED IN GROUND SLAB

Next, the analysis of pre-tensioning effects by the wire-winding of the cylindrical water tank based on a circular slab was carried out. The influence of pre-tensioning was taken into account as an axi-symmetrical pressure normal to the external surface of the shell with a trapezoidal profile in the vertical direction (see Fig. 9). This kind of radial pressure also models post-tensioning by cables, but rather in an approximate way. The PC tank dimensions were assumed as in the previous example, and, in addition, external pressure with trapezoidal distribution of pre-tensioning with the maximum and minimum pre-tensioning pressure: 50 kPa and 10 kPa, respectively. The load of the ground slab with the dead weight of the wall, as in p. 4.1, was also taken into account. The graphs of the radial displacements and the latitudinal moment in the shell are not included due to their analogy to the diagrams of the circumferential forces and the meridional moments, respectively. The plots which show the distributions of the circumferential forces N_ϑ and meridional moments M_z in the tank shell from the pre-tensioning pressure in the case of the substrate model in the form of the elastic half-space and two-parameter Winkler model are given in Fig. 12a) and b).

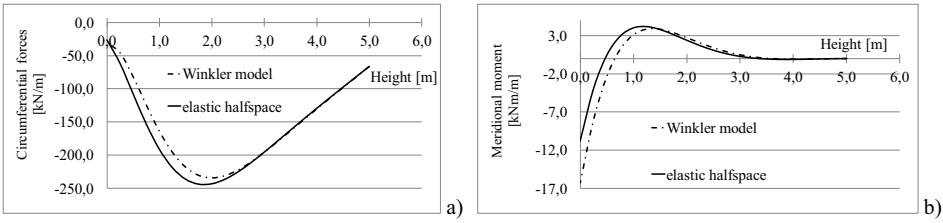

Fig. 12. Distributions of circumferential forces N_ϑ (a)) and meridional moments M_z (b)) in the tank wall from the prestressing pressure for the subsoil models of the elastic half-space and two-parameter Winkler model.

Then a superposition of the effects of actions on the structure was carried out, taking into account the graphs concerning particular load cases (liquid pressure, pre-tensioning). The diagrams which present the distributions of the hoop forces N_ϑ and meridional moments M_z in the shell from the combined hydrostatic pressure and pre-tensioning in case of the substrate model of an elastic half-space and two-parameter Winkler model are shown in Fig. 13a) and b). The plot in Fig. 13a) is not a

superposition of graphs in Figures 11a) and 12a), and the plot in Fig. 13b) is not a superposition of graphs in Figures 11b) and 12b), for the same reasons, as in the instance of PC silo (see p. 3.2).

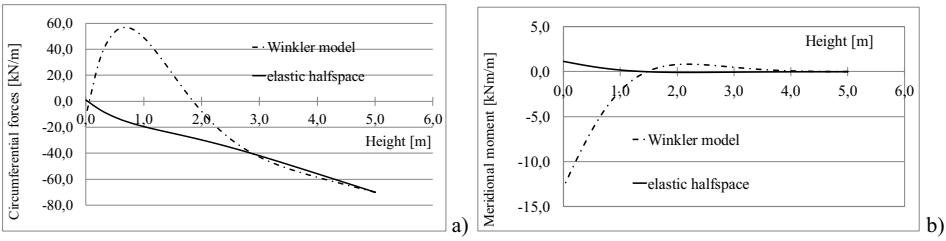

Fig. 13. Distributions of hoop forces N_ϑ (a)) and meridional moments M_z (b)) in the tank wall from the hydrostatic pressure and pre-tensioning for elastic half-space and two-parameter Winkler model for subsoil.

5. ANALYSIS OF RESULTS AND CONCLUSIONS

Considering two elastic subsoil models, it can be stated that the assumption of the substrate as an elastic half-space led in the examples to a different distribution of internal forces in silos and tanks in relation to the ground slab supported on the Winkler foundation. In the case of the elastic half-space model, a local nearly unrestricted increase of the substrate reaction around the circumference of the slab can be observed, unlike in the Winkler model. A lack of convergence of the soil reaction on the perimeter of the slab is justified within the framework of the theory of elasticity. In fact, local plasticizing of the substrate will occur (see [13]). The differences in the moment of attachment of the shell (A) result from the different behaviour of the ground slab, as described above. The slab resting on the elastic half-space is bent from the uniformly distributed load and edge forces, which effects in case of the silo A mutually cancel each other, and the slab settles almost evenly, while the same structure on the Winkler foundation is bent only from the edge forces, which is manifested by the larger absolute values of the moments in the slab at the junction with cylindrical shell. However, the effect of the foundation model is smaller in the case of pre-tensioning than in the case of the stored bulk material or liquid pressure. In the case of the external prestressing the ground slab is not loaded, so the main reason for the different behaviour of the structure for the two ground models disappears. Similarly, as a result of such an analysis of the RC water tank, much smaller radial displacements of the shell in the vicinity of the ground slab and substantially different bending moment diagrams were obtained compared to the Winkler model assumption. Due to different types and conditions of the subsoil and groundwater levels, it is not possible to certainly estimate which subsoil model is closer

to reality. The author recommends considering different cases, if necessary with the help of a non-linear FEM analysis of the task [14]. From the calculation examples of both prestressed concrete silos A and B, similar conclusions arise. Both in the case of the silo B based on the foundation ring and silo A based on the ground slab, a positive pre-tensioning effect in the form of a significant reduction of stress resultants applies to the upper part of the silo shell - about 90% of the shell height. For the remaining 10% the additional measures are required, which may take the form of significant thickening of the wall. Similarly, the computational example of the prestressed concrete tank shows that the positive pre-tensioning effect applies only to the top part of the shell - about 70% of the shell height. On the remaining 30% of its height, due to boundary disturbances, additional or alternative structural measures are necessary.

REFERENCES

1. H. Borowicka, “Druckverteilung unter elastischen Platten“, Ingenieur Archiv, X. Band: 113-125, 1939.
2. W. Flügge, “Stresses in Shells”, Second ed., Springer, Berlin, Heidelberg, 1973.
3. C. V. Girija Vallabhan, Y. C. Das, “Analysis of Circular Tank Foundations”, Journal of Engineering Mechanics, 117(4): 789-797, 1991.
4. M. I. Gorbunov-Posadov, T. A. Malikova, V. I. Solomin, “Calculation of structures on elastic foundation” (in Russian), Stroyizdat, Moskva, 1984.
5. J. A. Hemsley (Ed.), “Design applications of raft foundations”, Thomas Telford Publishing, London, 2000.
6. J. A. Hemsley, “Elastic analysis of raft foundations”, Thomas Telford Publishing, London, 1998.
7. J. S. Horvath, R. J. Colasanti, “Practical Subgrade Model for Improved Soil-Structure Interaction Analysis: Model Development”, International Journal of Geomechanics 11(1): 59–64, 2011.
8. Z. Kączkowski, “Plates. Static calculations”, (in Polish), Arkady, Warszawa, 2000.
9. A. R. Kukreti, M. M. Zaman, A. Issa, “Analysis of fluid storage tanks including foundation-superstructure interaction”, Applied Mathematical Modelling 17: 618-631, December 1993.
10. A. R. Kukreti, Z. A. Siddiqi, “Analysis of fluid storage tanks including foundation-superstructure interaction using differential quadrature method”, Applied Mathematical Modelling 21: 193-205, April 1997.
11. P. M. Lewiński, “Analysis of interaction of reinforced concrete and prestressed concrete cylindrical silo structures with soil”. SSTA2013 10th Conference: Shell Structures: Theory and Applications, 16-18 October, Gdańsk, Poland, pp. 547-550, 2013.
12. P. M. Lewiński, M. Rak, “Soil-structure interaction of cylindrical water tanks with linearly varying wall thickness”, PCM-CMM-2015: 3rd Polish Congress of Mechanics & 21st Computer Methods in Mechanics, 8-11 September, Vol. 2, Gdańsk, Poland, pp. 921-922, 2015.
13. P. Lewiński, “Analysis of interaction of RC cylindrical tanks with subsoil” (in Polish), Prace Naukowe ITB, Rozprawy, Wydawnictwa ITB, Warszawa, 2007.
14. P. M. Lewiński, S. Dudziak, “Nonlinear Interaction Analysis of RC Cylindrical Tank with Subsoil by Adopting Two Kinds of Constitutive Models for Ground and Structure”, American Institute of Physics, AIP Conference Proceedings 1922, 130007, 2018.
15. Z. E. Mazurkiewicz, (T. Lewiński - Ed.), „Thin elastic shells” (in Polish), Oficyna Wydawnicza Politechniki Warszawskiej, Warszawa, 2004.
16. E. S. Melerski, “Design Analysis of Beams, Circular Plates and Cylindrical Tanks on Elastic Foundations”, Taylor & Francis Group, London, 2006.
17. N. el Mezaini, “Effects of Soil-Structure Interaction on the Analysis of Cylindrical Tanks”, Practice Periodical on Structural Design and Construction 11 (1): 50-57, February 2006.
18. Z. Mistríková, N. Jendželovský, “Static analysis of the cylindrical tank resting on various types of subsoil”, Journal of Civil Engineering and Management 18 (5): 744-751, 2012.
19. W. Nowacki, R. Dąbrowski, “Silos. Calculation methods and construction” (in Polish), BiA, Warszawa, 1955.

LIST OF FIGURES AND TABLES:

WYKAZ RYSUNKÓW I TABLIC:

WSPÓŁPRACA ŻELBETOWYCH I SPRĘŻONYCH SILOSÓW I ZBIORNIKÓW CYLINDRYCZNYCH Z PODŁOŻEM GRUNTOWYM

Słowa kluczowe: silosy, zbiorniki, konstrukcje sprężone, współpraca grunt-konstrukcja, półprzestrzeń sprężysta, model Winklera

STRESZCZENIE:

Przedmiotem niniejszej pracy jest analiza wpływu obwodowego sprężania na oddziaływanie silosów i zbiorników cylindrycznych z podłożem. Podłoże zamodelowano w postaci półprzestrzeni sprężystej i modelu Winklera. Zachowanie konstrukcji powłokowych żelbetowych i sprężonych silosów i zbiorników cylindrycznych, zwłaszcza płyt dennych oddziałujących z podłożem, zależy w dużej mierze od rozkładu reakcji podłoża na powierzchni fundamentu. Analizę tych konstrukcji ze ścianami zamocowanymi w kołowej płycie dennej i pierścieniu fundamentowym przeprowadzono z uwzględnieniem modelu półprzestrzeni sprężystej na podstawie metody Gorbunowa-Posadowa i dwuparametrowego modelu podłoża Winklera. Podano przykłady analiz dotyczących żelbetowych i sprężonych cylindrycznych silosów (rys. 1) i zbiorników (rys. 2) ze ścianami sztywno połączonymi z konstrukcjami fundamentów.

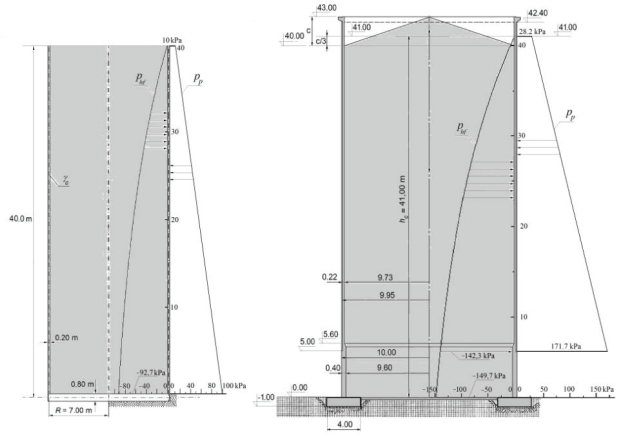

a) b)

Rys. 1. Silosy sprężone obrotowo-symetryczne: a) silos na zboże, b) silos tlenku glinu.

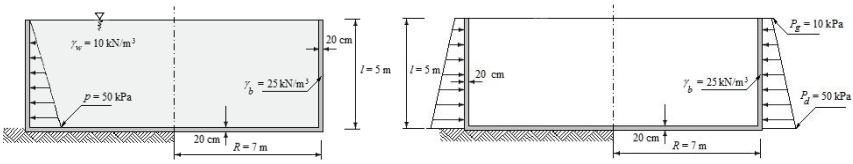

Rys. 2. Zbiornik cylindryczny na wodę i schemat obciążenia dociskiem od sprężenia o rozkładzie trapezowym.

Analizę opisanych konstrukcji przeprowadzono z uwzględnieniem izotropowej półprzestrzeni obciążonej prostopadle na pewnym obszarze płaszczyzny granicznej (tzn. zastosowano powierzchnię wpływu (funkcję Greena) przy użyciu

rozwiązania Boussinesqa) oraz równania różniczkowego płyty kołowej spoczywającej na półprzestrzeni sprężystej. Oprócz parcia typu Janssena i ciśnienia hydrostatycznego, uwzględniono wpływ docisku od wstępnego sprężenia o rozkładzie trapezowym. Uwzględniono także wpływ oddziaływania między płytą denną silosu lub zbiornika a podłożem w przypadku docisku od sprężenia wywieranego na powłokę. W p. 3 podano przykład ilustrujący, w jaki sposób założenie podłoża jako półprzestrzeni sprężystej prowadzi do innego rozkładu sił wewnętrznych w omawianych silosach niż w przypadku przyjęcia dwuparametrowego modelu Winklera, podczas gdy analiza oddziaływania cylindrycznych zbiorników na ciecze z podłożem przedstawiona jest w pkt. 4. Wykresy rozkładów sił wewnętrznych, tj. siły obwodowej N_ϑ i momentu południkowego M_z w powłoce silosu pokazanego na rys. 1a) od równoczesnego ciśnienia poziomego (p_{hf}) i wstępnego sprężenia dla modeli podłoża półprzestrzeni sprężystej i dwuparametrowego modelu Winklera pokazano na rys. 3, natomiast rozkłady tych sił powstałe w powłoce silosu pokazanego na rys. 1b) od równoczesnego ciśnienia poziomego (p_{hf}) i trapezoidalnego docisku od wstępnego sprężenia pokazano na rys. 4a) i b).

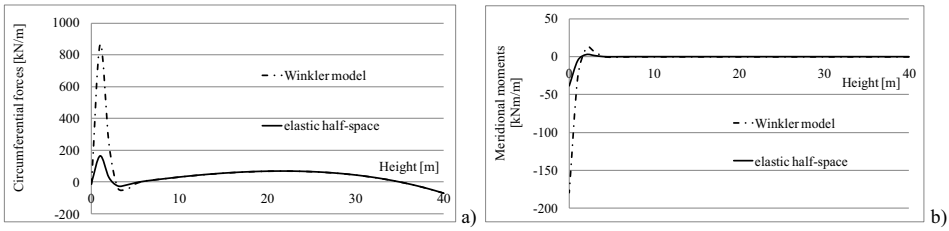

Rys.3. Rozkłady wypadkowe siły obwodowej N_ϑ (a)) oraz momentu południkowego M_z (b)) w powłoce silosu od parcia poziomego p_{hf} i od oddziaływań wstępnego sprężenia dla półprzestrzeni sprężystej i podłoża Winklera.

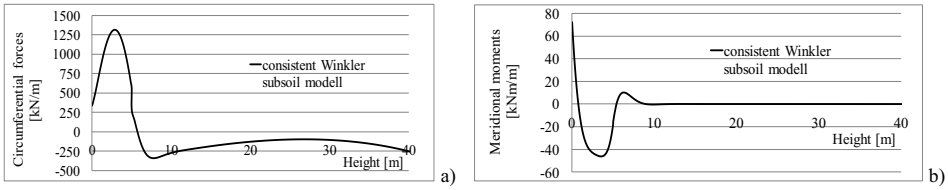

Rys. 4. Rozkłady wypadkowe siły obwodowej N_ϑ (a)) oraz momentu południkowego M_z (b)) w powłoce silosu od parcia poziomego p_{hf} i od oddziaływań wstępnego sprężenia.

Rozważając zbiorniki cylindryczne ze ścianami zamocowanymi w kołowej płycie dennej lub pierścieniu fundamentowym, określono końcowe efekty sprężenia uzyskane w wyniku superpozycji poszczególnych sił wewnętrznych. Zarówno w przypadku silosu opartego na pierścieniu fundamentowym, jak i na kołowej płycie dennej pozytywny efekt wstępnego sprężenia dotyczył tylko górnej części powłoki silosu - około jej 90% wysokości. Dla pozostałych 10% wymagane są dodatkowe zabiegi konstrukcyjne, które mogą przybrać formę np. znacznego pogrubienia ściany. Podobnie przykład obliczeniowy zbiornika z betonu sprężonego pokazuje, że dodatni efekt wstępnego sprężenia dotyczy tylko górnej części powłoki - około 70% jej wysokości. Chociaż wyniki dla obu modeli podłoża okazały się rozbieżne, poniższe wnioski są dość ważne dla praktyki inżynierskiej.

Received: 02.04.2020, Revised: 28.07.2020